

Spin injection characteristics of Py/graphene/Pt by gigahertz and terahertz magnetization dynamics driven by femtosecond laser pulse

Cite as: AIP Advances 11, 015321 (2021); <https://doi.org/10.1063/9.0000114>

Submitted: 15 October 2020 . Accepted: 25 November 2020 . Published Online: 08 January 2021

 H. Idzuchi,  S. Iihama, M. Shimura, A. Kumatani,  S. Mizukami, and Y. P. Chen



View Online

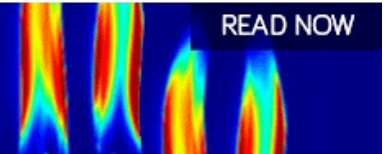


Export Citation



CrossMark

AIP Advances
Fluids and Plasmas Collection



Spin injection characteristics of Py/graphene/Pt by gigahertz and terahertz magnetization dynamics driven by femtosecond laser pulse

Cite as: AIP Advances 11, 015321 (2021); doi: 10.1063/9.0000114

Presented: 2 November 2020 • Submitted: 15 October 2020 •

Accepted: 25 November 2020 • Published Online: 8 January 2021



H. Idzuchi,^{1,2,3,a)} S. Iihama,^{4,5} M. Shimura,⁶ A. Kumatani,^{1,2,6,7} S. Mizukami,^{1,2,5} and Y. P. Chen^{1,2,3,5,8,9}

AFFILIATIONS

¹WPI Advanced Institute for Materials Research (AIMR), Tohoku University, Sendai 980-8577, Japan

²Center for Science and Innovation in Spintronics (CSIS), Tohoku University, Sendai 980-8577, Japan

³Department of Physics and Astronomy, Purdue Quantum Science and Engineering Institute, Purdue University, West Lafayette, Indiana 47907, USA

⁴Frontier Research Institute for Interdisciplinary Sciences (FRIS), Tohoku University, Sendai 980-8578, Japan

⁵Center for Spintronics Research Network (CSRN), Tohoku University, Sendai 980-8577, Japan

⁶Graduate School of Environmental Studies, Tohoku University, Sendai 980-8579, Japan

⁷WPI-International Center for Materials Nanoarchitectonics (MANA), National Institute for Material Science, Tsukuba 305-0044, Japan

⁸School of Electrical and Computer Engineering and Birck Nanotechnology Center, Purdue University, West Lafayette, Indiana 47907, USA

⁹Institute of Physics and Astronomy and Villum Center for Hybrid Quantum Materials and Devices, Aarhus University, 8000 Aarhus-C, Denmark

Note: This paper was presented at the 65th Annual Conference on Magnetism and Magnetic Materials.

a)Author to whom correspondence should be addressed: idzuchi@tohoku.ac.jp

ABSTRACT

Spin transport characteristics of graphene have been extensively studied so far. The spin transport along the *c*-axis is however reported by rather limited number of papers. We have studied spin transport characteristics through graphene along the *c*-axis with permalloy(Py)/graphene(Gr)/Pt by gigahertz (GHz) and terahertz (THz) magnetization dynamics driven by femtosecond laser pulses. The relatively simple sample structure does not require electrodes on the sample. The graphene layer was prepared by chemical vapor deposition and transferred on Pt film. The quality of the graphene layer was characterized by Raman microscopy. Time-resolved magneto-optical Kerr effect is used to characterize gigahertz magnetization dynamics. Magnetization precession is clearly observed both for Pt/Py and Pt/Gr/Py. The Gilbert damping constant of Pt/Py was 0.015, indicating a spin pumping effect from Py to Pt. The Gilbert damping constant of Pt/Gr/Py was found to be 0.011, indicating that the graphene layer blocks spin injection. We also performed the measurement of THz emission for Pt/Py and Pt/Gr/Py. While a THz emission is clearly observed for Pt/Py, a substantial reduction of THz emission is observed for Pt/Gr/Py. With these two different experiments, and highly anisotropic resistivity of graphite, we conclude that the vertical spin transport is strongly suppressed by the graphene layer.

© 2021 Author(s). All article content, except where otherwise noted, is licensed under a Creative Commons Attribution (CC BY) license (<http://creativecommons.org/licenses/by/4.0/>). <https://doi.org/10.1063/9.0000114>

Recently, two-dimensional (2D) materials have attracted considerable attention. Two-dimensional materials provide handful access to highly crystalline samples, offering new spintronics research directions. Since spin currents can flow in nonmagnetic materials, so far such spin transport has been widely studied in the in-plane direction of nonmagnetic 2D materials.^{1–3} In three-dimensional materials such as Pt, spin transport in the out-of-plane direction is often studied using the spin Hall effect. The spin current is converted to a charge transport with specific geometry: the spin polarization, flow direction of spin current, and direction of detection voltage all need to be perpendicular to each other. This geometrical constraint makes it difficult to study out-of-plane spin transport through the *c*-axis of 2D material due to the lack of relaxation volume in the thickness direction, while the in-plane spin transport has been relatively well studied. Here, we optically investigated spin transport characteristics in the *c*-axis of graphene using gigahertz (GHz) and terahertz (THz) magnetization dynamics excited by a femtosecond pulse laser. This makes it easier to satisfy such geometrical conditions as the injector and detector are not required to be electrically connected.

Figure 1 represents our sample structure as well as a brief measurement setup. Here, we employed spin pumping and THz emission, both induced by magnetization dynamics excited by a pulsed laser, as described below. Previously, vertical spin transport in multilayers of graphene has been studied by ferro magnetic resonance. Patra *et al.* fabricated the sample on a co-planer waveguide and used broadband frequency to characterize spin transport. They found that Gilbert damping is significantly enhanced for Py/Gr compared to Py/Pt where Py stands for permalloy ($\text{Ni}_{80}\text{Fe}_{20}$).⁴ Later, Gannett *et al.* studied a series of samples with different thicknesses of Py to characterize the transport properties, which shows no detectable enhancement for Py/Gr/Cu.⁵ While the interface of graphene can be complicated, in our experiment, the sample structure is simple (just a multilayer film). Complimentary characteristics were obtained by two methods, which should help reveal the intrinsic spin transport properties at the interface.

In this study, spin transport was studied on Pt/Gr/Py and Pt/Py. Pt, Gr, and Py were chosen for representative materials for spin Hall effect, 2D material, and soft ferromagnet. Pt film was prepared by sputtering with the thickness of 3 nm on silicon and glass substrates. The graphene film, with the dimension of approximately 8 mm by 8 mm, was transferred onto Pt in ambient conditions. Graphene film was prepared on thin copper foil by a standard chemical vapor deposition (CVD) method and transferred onto Pt film. Raman microscopy was used to characterize the number of layers in graphene with a 532-nm laser wavelength. We observed clear peaks of D, G, and 2D bands from left to right as shown in **Fig. 2a**. Particularly from the 2D peak, we confirmed the crystallinity of the graphene film and the film was not folded.^{6,7} The Py film and MgO capping layer was sputtered on the graphene film with a base pressure of $\sim 10^{-7}$ Torr. The static magnetization process of the film was examined by magneto optical Kerr effect. To measure GHz magnetization dynamics induced by the femtosecond laser pulse (**Fig. 1a**), a time-resolved magneto-optical Kerr effect (TRMOKE) was employed.⁸ The wavelength, pulse duration, and repetition rate for both the pump and probe laser pulses were 800 nm, 120 fs, and 1 kHz, respectively. The spot size of the pump and probe laser pulses used for TRMOKE measurement were 2.2 mm and 0.15 mm, respectively. The pump laser beam was irradiated on the sample from the film normal and the incident angle of the probe laser beam was ~ 5 degrees measured from the film normal. The Kerr rotation angle of the reflected probe beam was detected via a balanced photo-detector. The pump laser pulse was modulated by the mechanical chopper with a frequency of 360 Hz. Then the pump-laser induced change in the Kerr rotation angle was detected by a Lock-in amplifier. A magnetic field was applied with a 10-degree angle measured from the film normal. The magnetization precession can be excited by the reduction of a demagnetizing field due to laser heating. The damping of the magnetization precession reflects the transfer of spin into an adjacent normal metal layer, referred to as the spin-pumping effect.^{9,10} To study spin-transport induced by THz magnetization dynamics, THz time-domain spectroscopy was

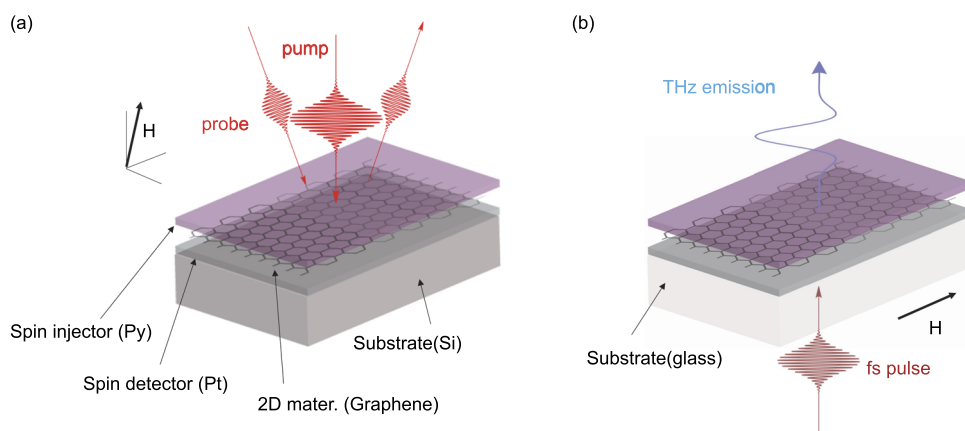


FIG. 1. Concept and schematic image of the experimental setup of this study. Graphene, the spin injector (Py) and detector (Pt) are depicted in a black hexagon, purple box, and gray box, respectively. (a) The setup for pump-probe measurement for magnetization dynamics. The probe beam is slightly (~ 5 deg) tilted from the film normal. The magnetic field is applied with a 10-degree angle measured from the film normal. (b) The setup for THz emission. The magnetic field is applied in-plane.

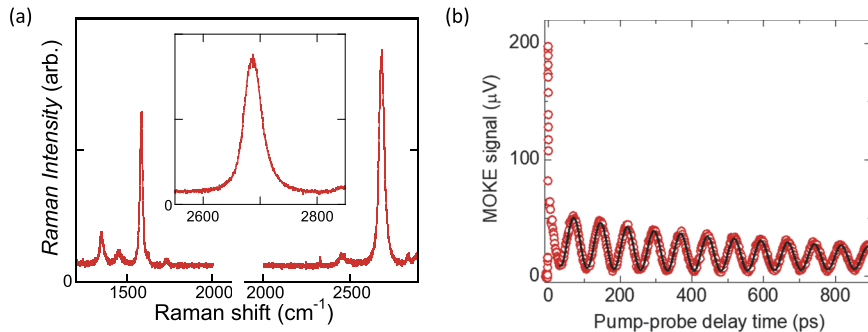


FIG. 2. (a) Raman spectroscopy of a graphene layer transferred on to a glass/Pt substrate (glass with Pt sputtered). Three main Raman peaks (D, G, and 2D) are clearly observed. Inset shows the 2D peak, clearly different from bilayer or multilayers graphene.⁶ (b) Magneto-optical Kerr effect (MOKE) signal plotted as a function of pump-probe delay time for Pt/Gr/Py(10nm)/MgO under an external magnetic field of 10.7 kOe. The field is applied with a 10-degree angle measured from the film normal. The measurement setup is schematically shown in Fig. 1a.

employed¹¹ (Fig. 1b), in which THz spin-current can be generated by ultrafast demagnetization of the Py layer and its angular momentum can be transferred to the Pt layer.^{12,13} Then, the THz electric field can be generated through spin-to-charge conversion (inverse spin Hall effect) in the Pt layer. The wavelength, pulse duration, repetition rate for the laser pulse were 800 nm, 120 fs, and 80 MHz, respectively. The femtosecond laser was irradiated from the substrate side and then THz electric field emitted from the film side was measured. The THz electric field was detected by an electro-optic sampling method using a ZnTe (110) crystal. All measurements were conducted at room temperature.

The spin transport of graphene in the vertical direction can be accessed by spin pumping with additional layers. We compared the Pt/Py bilayer with the Pt/Gr/Py trilayers in order to characterize spin transport properties across the graphene layer. Figure 2b shows a typical TRMOKE signal for Pt/Gr/Py(10nm)/MgO on Si substrate under the external magnetic field of 10.7 kOe in a direction tilted by 10 degrees from perpendicular to the substrate. We have

clearly observed spin precession slowly decaying over long period right after initial ultrafast dynamics, for the samples of both with and without graphene layer. Those oscillations are fitted to the following equations

$$A + B \cdot \exp(-vt) + C \cdot \exp(-t/\tau) \sin(2\pi ft + \phi_0),$$

where A , B , v , C , τ , and ϕ_0 are signal offset, the magnitude of exponential background signal due to the recovery of magnetization, decay rate, oscillation amplitude, oscillation frequency, oscillation lifetime, and initial phase, respectively. The TRMOKE signals are well fitted by the above equation shown as a solid curve in Fig. 2(b). The f and $1/\tau$ values were evaluated by fitting them with different applied magnetic fields as shown in Fig. 3. f and $1/\tau$ can be calculated theoretically using the Landau-Lifshitz Gilbert (LLG) equation as,^{8,14}

$$f_{\text{LLG}} = \frac{\gamma}{2\pi} \sqrt{H_1 H_2}, \quad (1)$$

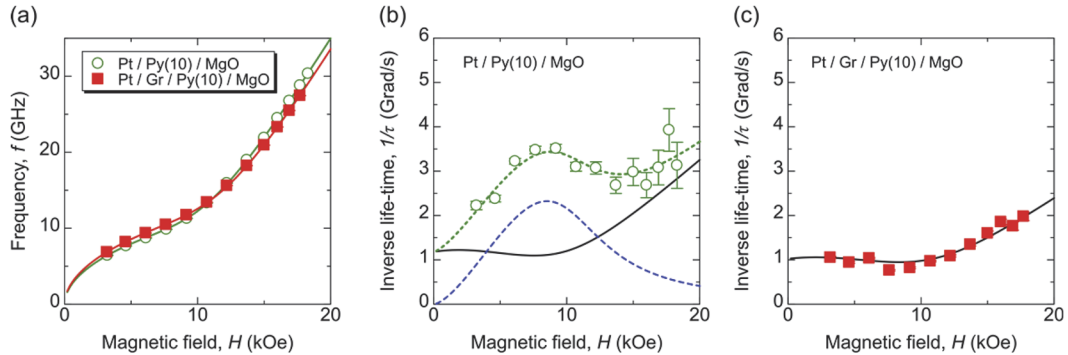


FIG. 3. Characterization of GHz magnetization dynamics for multilayers with and without graphene. The measurement setup is schematically shown in Fig. 1a. (a) precession frequency as a function of the magnetic field. The field is applied with a 10 degree angle measured from the film normal. Closed red squares and open green circles indicate data from the Pt/Gr/Py/MgO and Pt/Py/MgO respectively where the thickness of Py is 10 nm for both case. The solid curves are obtained by Eq. (1) with the parameters in the main text. Inverse lifetime as a function of the magnetic field for (b) Pt/Py/MgO and (c) Pt/Gr/Py/MgO films. The black solid curves shown in (b) and (c) correspond to the calculated value using LLG eq. (Eq. (2)). The green dotted and blue broken curves shown in (b) are the left hand side and the second term in the right hand side in Eq. (6), respectively, with the parameters in the main text.

$$\frac{1}{\tau_{LLG}} = \frac{1}{2} \alpha \gamma (H_1 + H_2), \quad (2)$$

$$H_1 = H \cos(\theta - \theta_H) - 4\pi M_{\text{eff}} \cos^2 \theta, \quad (3)$$

$$H_2 = H \cos(\theta - \theta_H) - 4\pi M_{\text{eff}} \cos 2\theta, \quad (4)$$

where H , θ_H (=10 degree in this study), θ , $4\pi M_{\text{eff}}$, γ , and α are external magnetic field, field angle, magnetization angle, effective demagnetizing field, gyromagnetic ratio and Gilbert damping constant respectively. γ is given by the relation, $\gamma = g\mu_B/\hbar$. The θ is determined by the minimum energy condition as,

$$H \sin(\theta_H - \theta) + 2\pi M_{\text{eff}} \sin 2\theta = 0, \quad (5)$$

The measured f is well fitted by Eq. (1) with the parameters $g = 2.09$ (2.06) and $4\pi M_{\text{eff}} = -9.8$ (-8.8) kOe for Pt/Gr/Py (Pt/Py) film. The $1/\tau$, calculated using Eq. (2), are shown in Fig. 3(b) and 3(c). $1/\tau$ for the Pt/Gr/Py/MgO sample (Fig. 3(c)) can be well explained by Eq. (2) with $\alpha = 0.011$. However, $1/\tau$ for Pt/Py/MgO cannot be explained by Eq. (2), which is due to inhomogeneous linewidth broadening. Therefore, $1/\tau$ enhancements due to inhomogeneous linewidth broadening are considered as follows,

$$\frac{1}{\tau_{\text{tot}}} = \frac{1}{\tau_{LLG}} + \frac{1}{2} \left| \frac{d(2\pi f_{LLG})}{d\theta_H} \right| \Delta\theta_H, \quad (6)$$

where, the first term is identical to Eq. (2) and the second term is $1/\tau$ enhancement due to the distribution of θ_H which may be related to the surface roughness of the film.¹⁴ The black solid and blue dashed curves in Fig. 3(b) are the calculated results of the first and second terms of Eq. (6). H_{ext} dependence of $1/\tau$ for the Pt/Py/MgO films is well explained by the summation of two contributions in Eq. (6) with the parameters, $\alpha = 0.015$ and $\Delta\theta_H = 0.05$ rad (green broken curve in Fig. 3(b)). The enhancement of α is due to spin-pumping effect at the Pt/Py interface associated with dissipation of angular momentum. This indicates strong suppression of spin current with graphene, consistent with Gannett *et al.*⁵ Previously, it was shown that graphene has a long spin diffusion length by means of lateral spin transport where the spin current is flowing in-plane with long spin lifetime probed by the Hanle effect.^{1,15} Transport along the *c*-direction can be rather different from the one in the *ab* plane. In early studies, graphite crystal showed rather anisotropic charge transport properties, and a larger resistivity of the *c*-axis was reported than the one of the *ab* plane by a factor of 10^2 to 10^3 .¹⁶ The resistive nature of the graphene along the *c* axis may prevent spin transport.

In the THz method, by irradiating a femtosecond laser pulse on this kind of multilayers, a THz electric field can be generated.^{12,13} Ultrafast spin current in nonmagnetic layers can be generated by the ultrafast demagnetization in the Py layer. Spin-charge conversion via the inverse spin-Hall effect in the Pt layer creates a terahertz charge current and electric field. In our bilayer Pt/Py, we observed a clear THz emission and its signal was inverted with a reversed bias magnetic field, as shown in Fig. 4(a). Interestingly, on two Pt/Gr/Py samples, the THz signal was largely suppressed (Fig. 4(b) and 4(c)). This implies a strong suppression of spin injection from Py to Pt by the Gr monolayer in the terahertz frequency range. The interpretation is qualitatively consistent with a spin pumping study (using ultrafast laser heating and GHz magnetization dynamics). The substantial

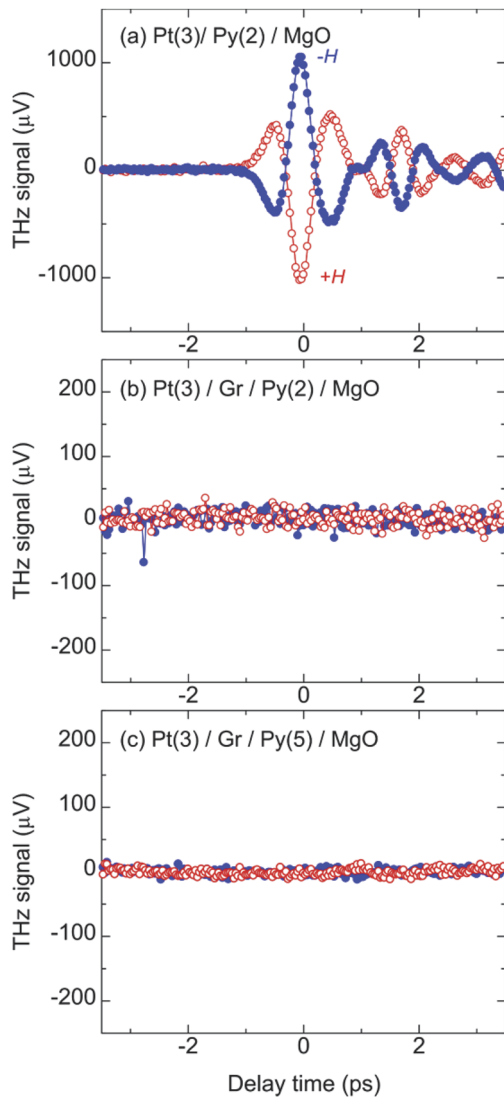


FIG. 4. Detection of THz electric field generated by femtosecond laser pulse on (a) Pt(3)/Py(2)/MgO, (b) Pt(3)/Gr/Py(2)/MgO and (c) Pt(3)/Gr/Py(5)/MgO made on glass substrates. The measurement setup is schematically shown in Fig. 1b. The numbers in the bracket indicate the thickness of the layers in the unit of nanometers. The magnetic field was applied in the in-plane direction. Blue solid and red open symbols are the signal obtained with the opposite magnetic field direction.

reduction of the THz signal is attributed to the strong suppression of spin-transport by inserting a graphene monolayer with a high resistivity along the *c*-axis. A substantial reduction of THz emission was also reported for Co/ZnO/Pt junctions.¹⁷ Using these two different characterization methods, we conclude graphene monolayer effectively blocks vertical spin current. For the second sample of Pt/Gr/Py (Fig. 4c), a small peak appeared around 1 ps. We notice this may or may not be a delayed THz emission, whose precise mechanism (e.g., how it may be related to the graphene barrier, whether it may also

be generated by Py itself etc.) is not clear at this stage and open for future study.

In conclusion, we have investigated the spin injection characteristics of Py/Gr/Pt by means of gigahertz and terahertz magnetization dynamics driven by a femtosecond laser pulse. The graphene layer was grown by CVD method, and the Raman characteristics on Pt showed the characteristics of single layer graphene film. We have clearly observed GHz magnetization precession induced by the laser pulse for the samples of both with and without graphene (Py/Pt). Graphene is observed to give an apparent suppression of the damping enhancement due to the spin-pumping effect at the Py/Pt interface, indicating a reduction of angular momentum dissipation by a graphene monolayer. The THz emission induced by the femtosecond laser pulse was observed for the Py/Pt bilayer, while the THz emission was strongly suppressed for Py/Gr/Pt, which clearly indicates that graphene blocks spin current in transport along the *c*-axis. Both experiments on spin pumping and the THz method can be understood by the strongly suppressed spin transport across the graphene layer.

AUTHORS' CONTRIBUTIONS

H.I. and S.I. contributed equally to this work.

ACKNOWLEDGMENTS

We acknowledge technical help from the AIMR common equipment unit. This work was supported in part by Advanced Institute for Materials Research (AIMR) under World Premier

International Research Center Initiative (WPI) of MEXT, Japan, and by AIMR fusion research program, by the Mazda Foundation, and by a Grant-in-Aid for Scientific Research from the Ministry of Education, Culture, Sports, Science and Technology (MEXT), JSPS KAKENHI (Grant Number 18H03858, 18H04473, 20H04623, and 20K14399).

DATA AVAILABILITY

The data that support the findings of this study are available from the corresponding author upon reasonable request.

REFERENCES

- ¹N. Tombros *et al.*, *Nature* **448**, 571 (2007).
- ²Y. P. Liu *et al.*, *Appl. Phys. Lett.* **102**, 033105 (2013).
- ³H. Idzuchi, A. Fert, and Y. Otani, *Phys. Rev. B* **91**, 241407 (2015).
- ⁴A. K. Patra *et al.*, *Appl. Phys. Lett.* **101**, 162407 (2012).
- ⁵W. Gannett *et al.*, *J. Appl. Phys.* **117**, 213907 (2015).
- ⁶L. M. Malard *et al.*, *Phys. Rep.* **473**, 51 (2009).
- ⁷A. C. Ferrari and D. M. Basko, *Nat. Nanotech.* **8**, 235 (2013).
- ⁸S. Iihama *et al.*, *Phys. Rev. B* **89**, 174416 (2014).
- ⁹Y. Tserkovnyak *et al.*, *Phys. Rev. Lett.* **88**, 117601 (2002).
- ¹⁰S. Mizukami *et al.*, *Phys. Rev. B* **66**, 104413 (2002).
- ¹¹Y. Sasaki *et al.*, *Appl. Phys. Lett.* **111**, 102401 (2017).
- ¹²T. Kampfrath *et al.*, *Nat. Nanotech.* **8**, 256 (2013).
- ¹³T. Seifert *et al.*, *Nat. Photon.* **10**, 483 (2016).
- ¹⁴S. Mizukami *et al.*, *Jpn. J. Appl. Phys.* **40**, 580 (2001).
- ¹⁵D. Khokhriakov *et al.*, *Carbon* **161**, 892 (2020).
- ¹⁶W. Primak and L. H. Fuchs, *Phys. Rev.* **95**, 22 (1954).
- ¹⁷G. Li *et al.*, *J. Phys. D: Appl. Phys.* **51**, 134001 (2018).